Colloid and Polymer Science (2018) 296:995–1003
https://doi.org/10.1007/s00396-018-4318-7

ORIGINAL CONTRIBUTION

Poly(amino acid)-based nanogel by horseradish peroxidase catalyzed crosslinking in an inverse miniemulsion

Šálek Petr[1] · Dvořáková Jana[1] · Černoch Peter[1] · Pavlova Ewa[1] · Proks Vladimír[1]

Received: 8 January 2018 / Revised: 23 March 2018 / Accepted: 23 March 2018 / Published online: 11 April 2018

Abstract

We present an investigation of horseradish peroxidase (HRP)/H_2O_2-mediated crosslinking in an inverse miniemulsion for the successful preparation of a stable colloidal nanogel from a poly(amino acid)-based polymer precursor. The precursor was obtained by the aminolysis of polysuccinimide with aminoethan-2-ol and tyramine, resulting in a poly(α,β-*N*-(2-hydroxyethyl)-D,L-aspartamide-*co*-*N*-(2-(4-hydroxyphenyl)ethyl)-D,L-aspartamide) polymer (PHEA-Tyr). Various concentrations of the PHEA-Tyr in aqueous solution with HRP were emulsified in the presence of cyclohexane and SPAN 80. The addition of a hydrogen peroxide solution induced crosslinking between the polymer chains via the phenol groups (Tyr) and targeted nanogel formation. The hydrodynamic radii (R_h^0), mean size documented by hydrodynamic radius (R_h), and morphology of the nanoparticles were investigated by dynamic light scattering (DLS) measurements, nanoparticle tracking analysis (NTA), and cryogenic transmission electron microscopy (cryo-TEM). It was found out that nanoparticle radius, morphology, and architecture of the nanogel could be regulated by the initial concentration of the precursor.

Keywords Enzymatic crosslinking · Inverse miniemulsion · Nanogel · Polyaspartamide

Introduction

Nanogels are widely studied nanomaterials since they integrate distinctive and unique properties of hydrogels and nanoparticles [1]. These nanoparticles with three-dimensional networks have been of great interest due to their favorable characteristics, including proper size, swelling in aqueous media, porosity, softness, stimuli-responsive behavior, hydrophilicity, degradability, and biocompatibility [2]. These new types of nanoparticles have also gained significant attention for their large surface area for bioconjugation and their internal network for cell encapsulation and incorporation of inorganic nanoparticles or biomolecules, such as DNA, peptides, and proteins. Thus, they are attractive for applications in drug delivery, tissue engineering, bionanotechnology, bioimaging, sensing, antifouling, etc. [3, 4].

✉ Šálek Petr
salek@imc.cas.cz

[1] Institute of Macromolecular Chemistry, Academy of Sciences of the Czech Republic, Heyrovsky Sq. 2, 162 06 Prague 6, Czech Republic

Nanogel synthesis can be based on natural materials, for example, chitosan, dextran, and proteins, or synthetic monomers and polymers or on their combination, including acrylic acid, *N*-isopropylacrylamide, 2-(dimethylamino) ethyl methacrylate, methoxydiethylene glycol methacrylate, aminoethyl methacrylamide hydrochloride, oligo(ethylene glycol) monomethyl ether methacrylate, and poly(ethylene glycol) dimethacrylate [5–12]. As is evident from the term "nanogel," the polymer chains of the nanoparticles are physically or chemically crosslinked to form the interior network between macromolecular chains [13]. Physical crosslinking comprises relatively weak non-covalent interactions between polymer chains, including hydrogen bonds, hydrophobic interactions, or ionic interactions, whereas chemically crosslinked polymer chains are joined covalently by various approaches. Examples include an addition of crosslinking monomer during polymerization, click chemistry, and enzyme-mediated crosslinking [1].

Neamtu et al. simply classified the preparation of nanogels into two groups: top-down and bottom-up approaches [7]. The process in which nanoparticles are synthetized from larger materials by physical, chemical, or mechanical degradation is called the top-down approach. Bottom-up nanogels are prepared from monomers or polymer precursors. The latter

method usually employs free or controlled radical polymerization adopting inverse miniemulsion, inverse microemulsion, precipitation, reversible addition fragmentation chain transfer, or atom transfer radical polymerization, as well as their combinations [14–20]. For example, conventional inverse miniemulsion polymerization is a suitable technique for the preparation of ~100–500-nm hydrophilic latexes in diameter from 2-hydroxyethyl methacrylate, acrylamide, and *N*-isopropylacrylamide. Briefly, the liquid monomer phase is dispersed into small droplets in a continuous organic phase using a high-energy input, such as a sonifier, in the presence of a hydrophobic emulsifier and osmotic agent to retard the diffusional degradation of the miniemulsion. The monomer droplets serve as the main polymerization locus [21, 22].

Due to fact that hydrogels based on amino acids or synthetic poly(amino acids) have suitable properties for biomedical applications and tissue engineering, they are also very promising for the preparation of hydrophilic crosslinked nanostructures [23, 24]. For example, Park et al. synthetized a poly(ethylene glycol)-grafted poly(succinimide) nanogel to analyze cellular uptake [25]. Furthermore, the triclosan-loaded, L-lysine-based nanogel prepared by a top-down approach showed antibacterial activity against some pathogens [26]. Additionally, linear water-soluble polymers based on synthetic poly(amino acids), such as poly(α,β-*N*-(2-hydroxyethyl)-D,L-aspartamide) (PHEA), meet all the requirements for preparation of hydrogels in terms of hydrophilicity, non-cytotoxicity, and biocompatibility and are generally used as model systems for their non-degradability [27–30]. In case that poly(amino acid)-based polymers bear functional groups on their chains, such as aromatic phenols, amines, or phenolic acids, they can easily form crosslinked structures via horseradish peroxidase (HRP)-catalyzed reaction [31]. The HRP catalyzes a decomposition of hydrogen peroxide (H_2O_2) in presence of reducing substrate (e.g., phenolic substrates) which is converted to radical product. One equivalent of H_2O_2 induces the formation of two aromatic radicals which are readily coupled by covalent bond to form crosslinked structure under mild conditions.

Herein, we report a combination of inverse miniemulsion and HRP/H_2O_2-mediated crosslinking for the preparation of a hydrophilic and colloidal stable nanogel. The poly(α,β-*N*-(2-hydroxyethyl)-D,L-aspartamide-*co*-*N*-(2-(4-hydroxyphenyl)ethyl)-D,L-aspartamide) (PHEA-Tyr) was initially obtained by aminolysis of polysuccinimide (PSI) and was used as a polymer precursor for the bottom-up synthesis at different concentrations. By taking advantage of PHEA-Tyr behavior in water solutions, the combination of inverse miniemulsion and HRP/H_2O_2-mediated crosslinking resulted in water-stable colloidal nanogels. The particles were then investigated by dynamic light scattering (DLS), nanoparticle tracking analysis (NTA), and cryogenic transmission electron microscopy (cryo-TEM); the obtained nanogels had different radii and morphology varying from globule-composed to low-crosslinked, hydrogel-related structures depending on PHEA-Tyr concentration.

Materials and methods

Materials

N,*N*-dimethylformamide (DMF) and cyclohexane (CHX) were purchased from Lach-Ner (Czech Republic). Aminoethan-2-ol (Fluka) was purified by vacuum distillation. Tyramine, hydrogen peroxide solution 30% (*w*/*w*) in water, peroxidase from horseradish (type VI), and sorbitane monooleate (Span 80) were purchased from Sigma-Aldrich and were used without further purification. PSI with M_w ~30,000 was obtained from F. Rypáček (Institute of Macromolecular Chemistry, Academy of Sciences of the Czech Republic, Heyrovsky Sq. 2, 162 06 Prague 6, Czech Republic). It was prepared from D,L-aspartic acid (Loba Chemie, Wien, analytical grade) by thermal polycondensation in the presence of phosphoric acid according to Neri et al. [32].

Synthesis of the polymeric gel precursor PHEA-Tyr

The PHEA-Tyr gel precursor was prepared from PSI through stepwise aminolysis using tyramine and aminoethan-2-ol in DMF (Scheme 1). Briefly, PSI (10 g, 0.103 mol) was dissolved in DMF (250 mL), then the tyramine was added (2.82 g, 0.0206 mol), and reaction mixture was stirred at room temperature for 24 h. Subsequently, the residual PSI groups were aminolyzed with aminoethan-2-ol (8 g, 0.1310 mol) to obtain a water-soluble polymer PHEA-Tyr. The reaction was carried out for 5 days at room temperature. The resulting polymer was purified by dialysis (molecular weight cutoff < 3000 Da) successively against a 100 mM sodium chloride solution for 2 days, a mixture of distilled water and ethanol (3:1) for 1 day, and distilled water for 2 day. The purified solution was lyophilized to obtain PHEA-Tyr with a yield of 53%.

Gel permeation chromatography (GPC) was performed on a system (Knauer) equipped with a diode array detection (DAD; wavelengths 205, 254, and 280 nm), an evaporative light scattering detection (ELSD) (Altech 3300, Grace, USA), and Phenomenex PolySep™-SEC GFC-P Linear Column 300 × 7.8 mm using a mixture of 0.05 M ammonia acetate buffer, pH 6.5/acetonitrile 80:20 as the eluent at the flow rate of 0.3 mL/min. The system was calibrated with polyethylene oxide standards.

Scheme 1 Aminolysis of polysuccinimide with tyramine and aminoethan-2-ol

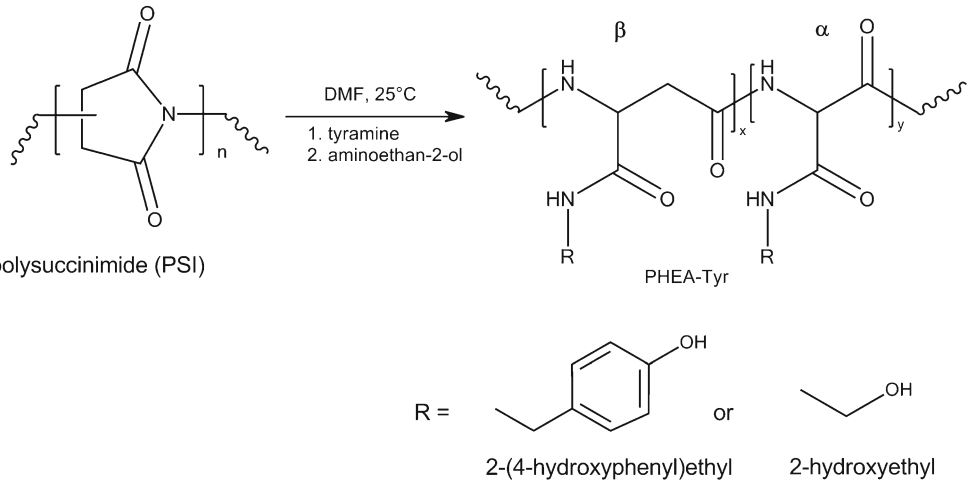

The degree of tyramine substitution of PHEA-Tyr was determined using UV-Vis spectrometry (Specord 250 Plus, Analytik Jena AG, Germany).

The presence of covalently bonded tyramine units was confirmed by the GPC measurements using the DAD detector and by ^{1}H-NMR (Bruker 300 MHz, D_2O, δ, ppm): 6.99 (d, 2H), 6.65 (d, 2H), 4.64 (m, 1H, NH-CH-CO), 3.41 (s, 2H, $NHCH_2CH_2OH$), 3.13 (s, 2H, $NgHCH_2CH_2OH$), 2.57 (s, 2H, $NHCHCH_2CO$), 2.50 (s, 2H, $CHCH_2CO$).

Preparation of PHEA-Tyr nanogel in inverse miniemulsion

Preparation of PHEA-Tyr nanogels in inverse emulsion was carried out in a 30-mL glass reaction vessel equipped with an anchor-type stirrer. In a typical experiment, PHEA-Tyr (0.18 g) and NaCl (0.263 g) were dissolved in water (4.32 g). Simultaneously, Span 80 (0.655 mL) was dissolved in cyclohexane (20.4 g). Then, both solutions were mixed together and horseradish peroxidase (0.1 mg) was added into to mixture. The mixture was cooled at 0 °C and sonicated using a W-385 sonicator (Heat System Ultrasonics; Farmingdale, NY) for 150 s at amplitude 50%. The dispersion was transferred into the glass reaction vessel under stirring (500 rpm) and hydrogen peroxide (11.25 μL) was added, and the reaction was allowed to proceed at 25 °C for 18 h. At the end of the reaction, PHEA-Tyr nanogel was removed by centrifugation (9000 rpm) and washed with methanol, ethanol, and water. Then, the nanogels were purified by dialysis (molecular weight cutoff < 3000 Da) against ethanol/distilled water mixture (1:1) for 48 h and against distilled water for 24 h. Methanol, ethanol, and water were used to remove unreacted components such as cyclohexane, SPAN 80, and unreacted PHEA-Tyr. The nanogels were finally freeze-dried from water.

DLS

Dispersions of nanoparticles were investigated by dynamic light scattering (DLS) using ALV-6010 correlator equipped with an ALV/CGS-8F goniometer, a 22-mW He-Ne laser (wavelength $\lambda = 632.8$ nm), and pair of avalanche photodiodes operated in a pseudo-cross-correlation mode. The measured intensity correlation function $g^2(t)$ was analyzed using the algorithm REPES [33] performing the inverse Laplace transformation according to

$$g^2(t) = 1 + \beta\left[\int A(t)\exp(-t/\tau)d\tau\right]^2 = 1 + \beta\left[\sum_{i=1}^{n} A_i\exp(-t/\tau_i)\right]^2,$$

where t is the delay time of the correlation function and β is an instrumental parameter and yielding distribution $A(\tau)$ of relaxation times τ. The relaxation time τ is related to the diffusion coefficient D and relaxation (decay) rate Γ by the relation:

$$\Gamma = \frac{1}{\tau} = D_q{}^2,$$

where q is the scattering vector defined as

$$q = \left(\frac{4\pi n}{\lambda}\right)\cdot\sin\left(\frac{\theta}{2}\right),$$

where n is the refractive index of the solvent and θ is the scattering angle. The hydrodynamic radius R_h of the particles can be calculated from the diffusion coefficient using the Stokes-Einstein equation:

$$D = \frac{k_B T}{6\pi\eta R_h},$$

where T is the absolute temperature, η is the viscosity of the solvent, and k_B is the Boltzmann constant. The hydrodynamic

radius R_h^0 of nanogels was obtained by subsequent double extrapolation of measured data to $q = 0$ and concentration $c = 0$ to compare obtained results with another method. In case of the initial droplets of polymer precursor in 1 M NaCl and the emulsion of polymer precursor in inversion emulsion, the DLS measurements were made at a 90° angle due to time instability of the analyzed samples and values of hydrodynamic radius R_h was obtained.

The samples for DLS measurement (5 mL; 1 mg/mL) were dispersed in Milli-Q water in glass vials by UP200S ultrasonic processor (Hielscher Ultrasonics GmbH, Teltow, Germany) for 5 min at intensity 50%, and 1 mL of each sample was used for the measurement.

NTA

NTA measurements were performed using a NanoSight NS300 (Malvern, Worcestershire, UK) containing a sample chamber of about 1 mL, 532-nm laser and camera sCMOS. The sample was pumped into the chamber with a sterile 1-mL syringe. Each sample was analyzed for 60 s and five times with manual adjustment, and all measurements were performed at 25 °C. The NTA 2.3 Dev Build 3.2.16 analytical software was used for data capturing and data evaluation.

The samples for NTA (5 mL; 1 mg/mL) were dispersed in Milli-Q water in glass vials by UP200S ultrasonic processor (Hielscher Ultrasonics GmbH, Teltow, Germany) for 5 min at intensity 50%. Then, each sample was diluted by Milli-Q water at concentration 10 μg/mL and about 0.8 mL of the sample was pumped into the chamber with a sterile 1-mL syringe.

cryo-TEM

Cryo-TEM observations were performed on a Tecnai G2 Spirit Twin 120 kV (FEI, Czech Republic), equipped with cryo-attachment (Gatan, cryo-specimen holder) using a bright-field (BF) imaging mode at accelerating voltage 120 kV.

Cryo-TEM allows direct investigation of samples in the vitrified, frozen-hydrated state.

The dispersion of each sample was applied to an electron microscopy grid covered with holey carbon-supporting film (300 MESH, Cu) after hydrophilization by glow discharge (Expanded Plasma Cleaner, Harrick Plasma, USA). The excess of the solution was removed by blotting (Whatman no. 1 filter paper) for ~1 s, and the grid was immediately plunged into liquid ethane held at − 182 °C. The frozen sample was immediately transferred into the microscope and observed at − 173 °C under the conditions described above.

The samples for cryo-TEM measurement (5 mL; 4 mg/mL) were dispersed in Milli-Q water in glass vials by UP200S ultrasonic processor (Hielscher Ultrasonics GmbH, Teltow, Germany) for 5 min at intensity 50%, and 3 μL of each sample was used for the measurement.

Results and discussions

First, PSI (M_w ~30,000) was converted into linear PHEA-Tyr by an aminolysis reaction (Scheme 1). The content of Tyr on the PHEA-Tyr polymer was determined to be 18.5 mol% by UV spectroscopy at 275 nm. The PHEA-Tyr polymer was analyzed with GPC, and it was found that the synthesized polymer had a dispersity of $Đ = 1.71$ and that the number average (M_n) and weight average (M_w) molecular weights were 7900 and 13,500, respectively.

The PHEA-Tyr was then used for the preparation of crosslinked nanoparticles with the assumption that linear PHEA exists in a random coil conformation in aqueous solution [34], which could contribute to the desired formation of spherical particles. Before the nanoparticle synthesis, the PHEA-Tyr solution in 1 M NaCl (1 mg/mL) was examined by DLS because the reaction environment for the preparation of the nanogels contains NaCl in this concentration. The results showed a bimodal intensity-based distribution, indicating the presence of clusters with R_h ~200 nm (ca. 20%) and small particles with R_h ~6 nm (ca. 80%). This result indicates that the majority of PHEA-Tyr polymer is present in molecularly dissolved form, which is visualized in Fig. 1 by the conversion of the measured intensity- to volume-based distribution. This observation is well correlated with the results of Coviello et al., who found that PHEA with a molecular weight $M_w = 52{,}000$ formed random coils with a radius of gyration of ~6 nm in aqueous solution [35].

The main objective of this work was to prepare crosslinked nanometer-sized hydrophilic particles from biocompatible

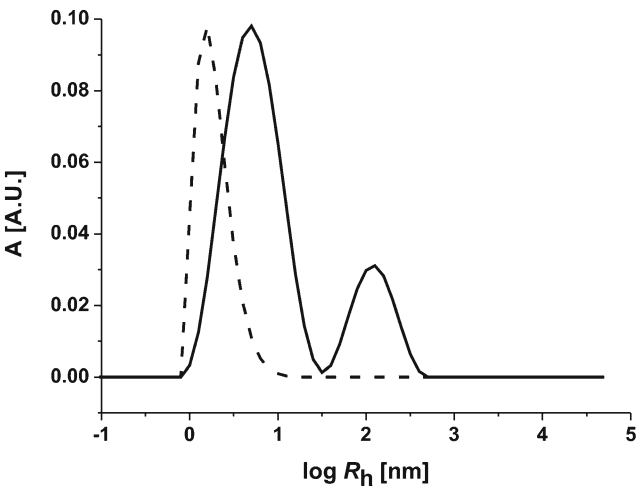

Fig. 1 DLS results of the examination of an aqueous solution of PHEA-Tyr as an intensity-based distribution (solid) and a volume-based distribution (dash)

PHEA-Tyr by enzymatic crosslinking in an inverse miniemulsion. The effect of various concentration of aqueous solution of PHEA-Tyr (4 to 12 wt%) in aqueous solution was investigated on the final particle size and morphology. As the first, the stable inverse miniemulsion consisting of PHEA-Tyr, water, HRP, CHX, SPAN 80, and NaCl, which acted as a lipophobe preventing the droplets from coalescence, known as Ostwald ripening, was obtained after the sonication procedure because it represented a crucial point of overall procedure [21]. The initial inverse miniemulsions were analyzed by DLS to obtain R_h values of the formed droplets which grew from 202 ± 15 to 357 ± 90 nm with increasing PHEA-Tyr concentration. Secondly, the formed inverse miniemulsion was transferred into a reactor, and while being vigorously stirred, the H_2O_2 was added to ensure an immediate formation of the nanogel. In this system, each droplet composed of the PHEA-Tyr random coils represented a small reactor. The introduction of H_2O_2 molecules into the droplet initiated the enzymatic covalent crosslinking between the globular coils and the formation of the intrinsic network within the nanoparticle. We assumed that H_2O_2 mainly acted as the crosslinking agent after penetration into the droplets when appeared on the oil-water interface and also during collision of the droplets. The resulting colloidally stable nanogels (NG1–5) were then purified, freeze-dried, and sonicated in water for further examination by DLS, NTA, and cryo-TEM.

The DLS analysis with double extrapolation of final NG1–5 nanogels demonstrated that the R_h^0 increased from 271 ± 5 to 449 ± 23 nm with increasing concentration of PHEA-Tyr in the miniemulsion (Table 1) as was observed with the sizes of initial emulsions. This observation suggested that at higher concentrations of PHEA-Tyr, the inverse miniemulsion with larger polymer precursor-based droplets were formed resulting in the larger final nanogel. The increase of polymer precursor concentration also led to formation on nanogels with broad particle size distribution.

Table 1 Summary of HRP-catalyzed crosslinking in inverse miniemulsion, DLS, and NTA measurements

Nanogel	PHEA-Tyr concentration (wt%)	R_h^0 of nanogels[a] (nm)	R_h of nanogel[b] (nm)	Conversion (%)
NG1	4	271 ± 5	158 ± 53	52
NG2	6	410 ± 23	186 ± 87	47
NG3	8	333 ± 10	165 ± 50	37
NG4	10	409 ± 31	231 ± 80	25
NG5	12	449 ± 23	266 ± 91	31

[a] Hydrodynamic radius R_h^0 was obtained by DLS with double extrapolation of measured data to $q = 0$ and concentration $c = 0$

[b] Mean hydrodynamic radius R_h was obtained by NTA from volume distribution

Although all DLS measurements of the original emulsions were performed at one angle and the measurement of nanogels with double extrapolation, it was possible to trace that the sizes of the nanogels were close to R_h of the corresponding inverse miniemulsion droplets. This could support our assumption that the sizes of final nanogels could be regulated by initial concentration polymer precursor and droplet size of starting inverse miniemulsion which was in agreement with theory about conventional miniemulsion polymerization when the average particle size is comparable to the original droplet size [36]. Due to the fact that the DLS measurements of the original emulsions were performed only at 90° angle, these values were not mentioned in Table 1.

The NG1–5 nanogels were further analyzed by NTA, because this analysis enables more accurate sizing and high resolution of particle size distribution compared to DLS and visualization of nanoparticles in dispersion [37]. The measurements confirmed that the R_h of the NG1–NG5 increased with increasing polymer precursor concentration (Table 1). However, the sizes collected by NTA were approximately two times lower than data obtained by DLS. The differences could be explained by the fact that DLS method is not sensitive in resolving of sample peak with broad size distribution, and the results can be affected by presence of larger particles which scatter the light more that smaller particles [37]. This effect may complicate the accurate sizing. Table 1 also includes the standard deviation (SD) values of the five independent measurements for each sample calculated by the NTA software. The SDs were rather high, indicating that sizes of NG1–5 were spread out over a wider range of values.

Contrary to the size of nanogels, the reaction conversion decreased with increasing PHEA-Tyr concentration in the dispersed phase (Table 1). This decline was explained by the fact that H_2O_2 was maintained at a constant concentration and thus always initiated a crosslinking of the same amount of the polymer precursor regardless of the increase of PHEA-Tyr concentration in the reaction feed. Therefore, more unreacted and non-crosslinked polymer precursor was removed during washing step in the case of HRP/H_2O_2-mediated crosslinking in inverse miniemulsion of PHEA-Tyr with the higher concentration.

Figure 2a–e demonstrates the NTA video frames of visualized and analyzed NG1–NG5 in aqueous dispersion. It was obvious that HRP/H_2O_2-mediated crosslinking of PHEA-Tyr polymer precursor in an inverse miniemulsion resulted in the nanoparticles which were individual and had broad size distribution. But our poly(amino acid)-based nanogels were insoluble in water and colloidally stable in aqueous dispersion because they did not form aggregates.

The cryo-TEM analysis was carried out to deeply investigate the architecture, morphology, and size of the purified nanoparticles. However, it is important to emphasize that the measurement was complicated due to the low contrast and

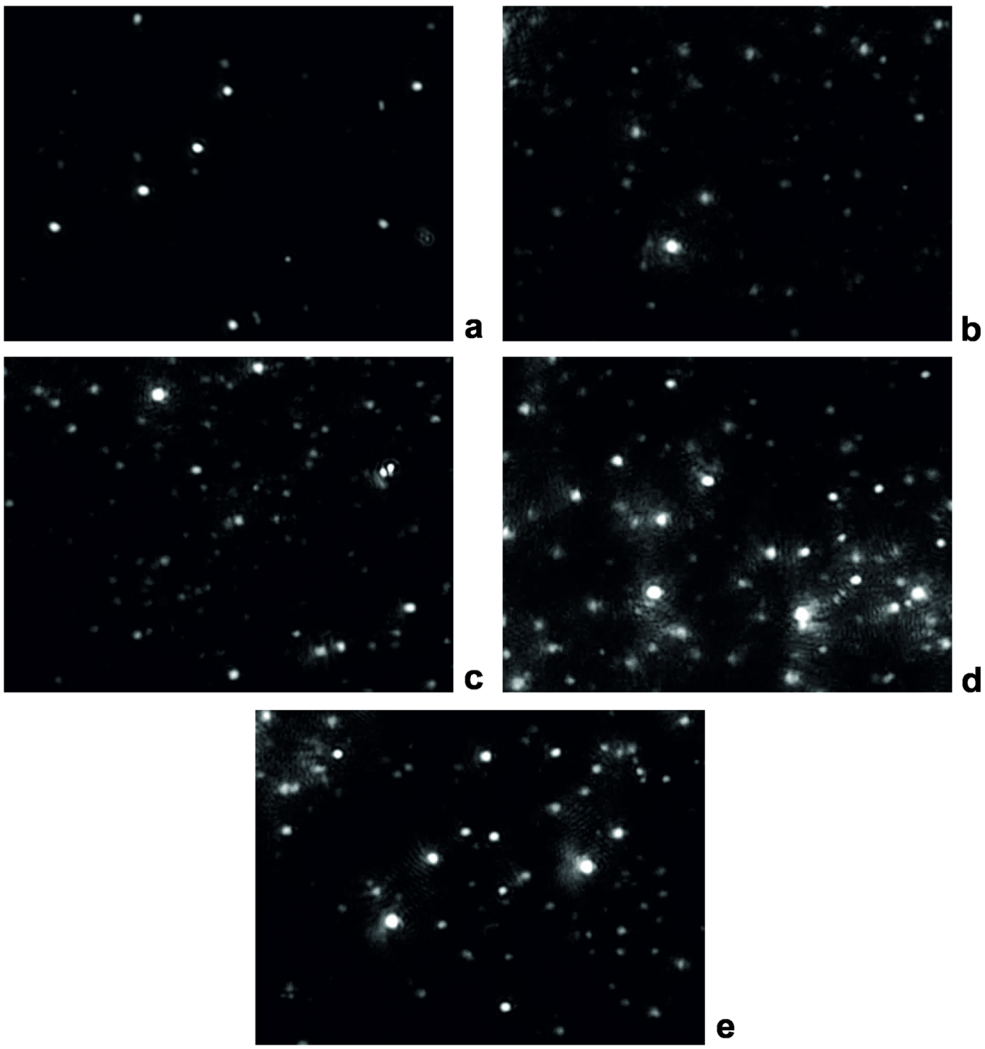

Fig. 2 NTA video frames of aqueous dispersions of (**a**) NG1 with mean R_h = 158 ± 53 nm, (**b**) NG2 with mean R_h = 186 ± 87 nm, (**c**) NG3 with mean R_h = 165 ± 50 nm, (**d**) NG4 with mean R_h = 231 ± 80 nm and (**e**) NG5 with mean R_h = 266 ± 91 nm prepared by HRP/H_2O_2-mediated crosslinking in an inverse miniemulsion. The analyses run for 60 s and were repeated five times with manual adjustment. All measurements were performed at 25 °C. Camera type sCMOS, Green laser type and camera level 13

softness of the nanogels. Therefore, we analyzed NG1 and NG5 nanogels which represented the most different samples in our set of experiments.

Figure 3a–f shows the cryo-TEM images of NG1 and NG5 nanogels, which confirmed that the combination of HRP/H_2O_2-mediated crosslinking in the inverse miniemulsion led to the successful formation of spherical nanoparticles from the PHEA-Tyr polymer precursor. The cryo-TEM images of NG1 nanoparticles (Fig. 3a, b) documented that prepared nanogel were spherical in shape and had compact structure, seemingly composed of the small ~5-nm globules corresponding to the PHEA-Tyr coils. This similarly composed architecture was also observed with elastin-like recombinamer nanogels [38]. Moreover, our finding was in agreement with the DLS measurement of solution of PHEA-Tyr in 1 M NaCl which contained the polymer coils with R_h ~6 nm. This also suggested our primary hypothesis about particle formation from the PHEA polymer precursor.

In contrast to NG1, the NG5 nanogel (Fig. 3c–f) was softer, contained large pores with the approximate radius from 20 to 70 nm, and its morphology resembled low HRP/H_2O_2-crosslinked poly(amino acid)-based hydrogels [39]. Our cryo-TEM observations proved that final architecture of the nanogels was strongly dependent on the initial concentration of PHE-Tyr polymer precursor. In case of 4 wt% of PHEA-Tyr, the miniemulsion contained smaller droplets and the addition of H_2O_2 induced the crosslinking of more polymer chains in each droplet resulting in less optically transparent NG1 nanogel with more rigid structure and less unreacted polymer precursor was removed during washing step. Also, Koul et al. observed that the interpenetrating polymer network nanogels composed of poly(acrylic acid) and gelatin with high cross-linked density prepared by inverse miniemulsion technique showed higher contrast during transmission electron microscopy [40]. In spite of that, less polymer chains were transformed into the crosslinked nanostructure when initial concentration of PHEA-Tyr was 12 wt%, and the obtained NG5 was larger with highly porous and soft structure, more optically transparent. Moreover, these hydrogel nanoparticles seemed to be lower crosslinked in

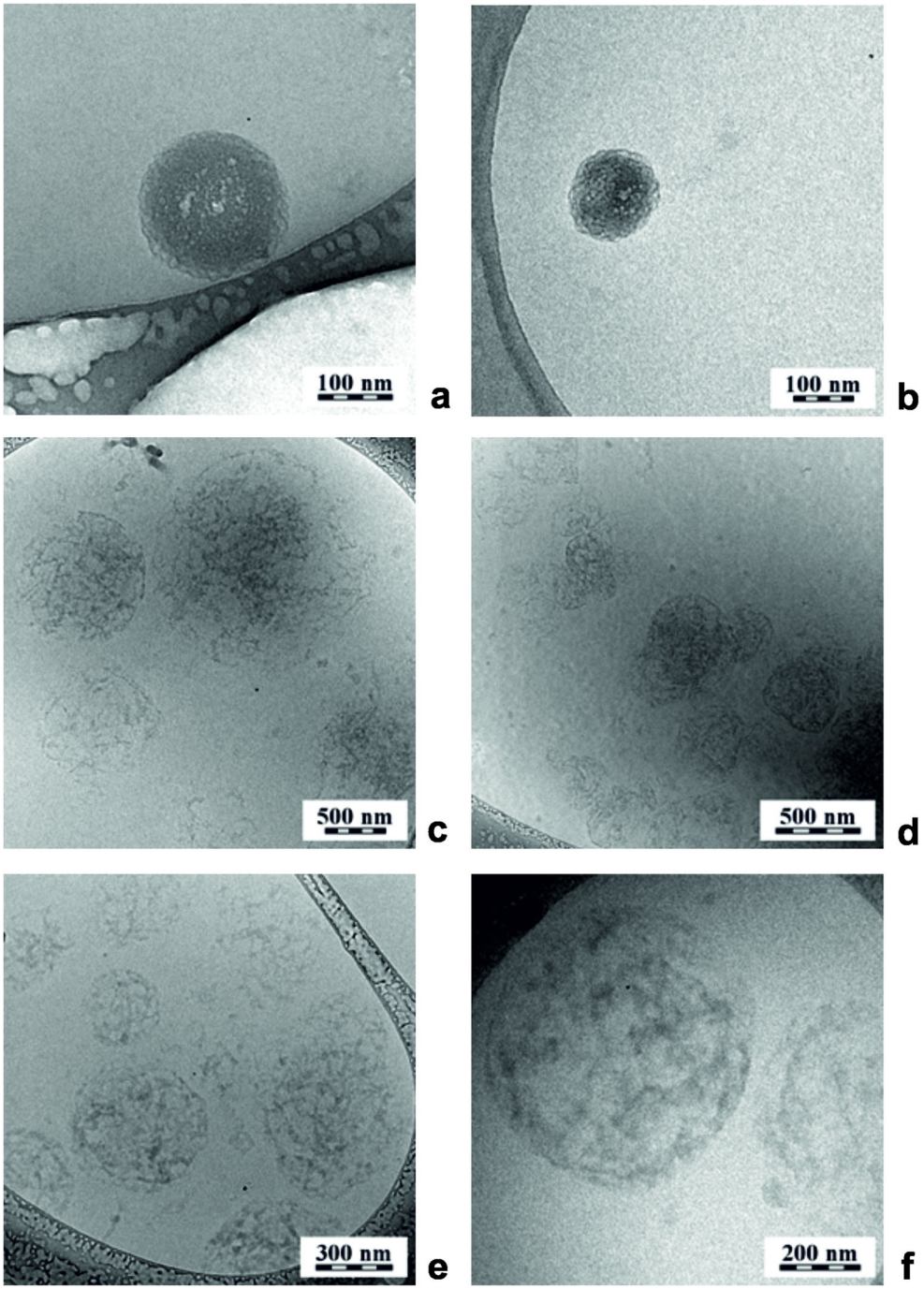

Fig. 3 Cryo-TEM images of NG1 (**a**, **b**) and NG5 (**c**–**f**) with different magnitudes

comparison with NG1 and structurally similar to low crosslinked hydrogels. Wu et al. described a preparation of ~200-nm polyglycerol nanogels in diameter with spherical shape and porous structure by HRP/H_2O_2-catalyzed crosslinking in inverse miniemulsion [41]. However, the authors stated that their porous nanogel was water-soluble, what seemed to be inconsistent with their conclusions. Despite the fact that our cryo-TEM images did not show a sufficient number of particles to analyze their average radius, the average size of the depicted NG5 particles was evaluated and found to be in range from 80 to 290 nm and average radius was 175 ± 58 nm.

Conclusions

In summary, we found that the two approaches, HRP/H_2O_2-mediated crosslinking and inverse miniemulsion technique, can be applied for the preparation of spherical and colloidal stable poly(amino acid)-based nanogels. By taking advantage

of PHEA-Tyr polymer precursor behavior in aqueous solution and knowledge of conventional inverse miniemulsion polymerization, the nanogels with various sizes and morphologies were prepared depending on initial concentration of the polymer precursor. The average R_h^0 values were determined by DLS and mean R_h by NTA. Both measurements showed that the size of the nanogels increased with the increasing concentration of the polymer precursor. The prepared nanogels were visualized by NTA confirming their colloidal stability in water and nanoparticle character. The architecture and morphology of the final nanogels varying from compact to soft and highly porous structures also depended on the initial concentration of the polymer precursor which was documented by cryo-TEM images. While these nanogels were prepared from a non-degradable precursor, this study provides an important background for subsequent synthesis of a poly(α,L-amino acid)-based biodegradable nanogel and proved the usefulness of the method to synthesize covalently crosslinked, colloidal stable nanoparticles from other polymer precursor with reactive functional groups.

Acknowledgments

Financial support from the Czech Science Foundation (No. 16-02702S) is gratefully acknowledged.

Compliance with ethical standards

Conflict of interest The authors declare that they have no competing interest.

References

1. Vinogradov S, Batrakova E, Kabanov A (1999) Poly(ethylene glycol)–polyethyleneimine nanogel™ particles: novel drug delivery systems for antisense oligonucleotides. Colloid Surf B 16:291–304
2. Soni KS, Desale SS, Bronich TK (2016) Nanogels: an overview of properties, biomedical applications and obstacles to clinical translation. J Control Release 240:109–126
3. Zhang X, Malhotra S, Molina M, Haag R (2015) Micro- and nanogels with labile crosslinks—from synthesis to biomedical applications. Chem Soc Rev 44:1948–1973
4. Iwasaki Y, Kondo JI, Kuzuya A, Moriyama R (2016) Crosslinked duplex DNA nanogels that target specified proteins. Sci Technol Adv Mat 17:285–292
5. Pujana MA, Pérez-Álvarez L, Iturbe LCC, Katime I (2012) Water dispersible pH-responsive chitosan nanogels modified with biocompatible crosslinking-agents. Polymer 53:3107–3116
6. Singh S, Möller M, Pich A (2013) Biohybrid nanogels. J Polym Sci Pol Chem 51:3044–3057
7. Neamtu I, Rusu AG, Diaconu A, Nita LE, Chiriac AP (2017) Basic concepts and recent advances in nanogels as carriers for medical application. Drug Deliv 24:539–557
8. Meléndez-Ortiz HI, Peralta RD, Bucio E, Zerrweck-Maldonado L (2014) Preparation of stimuli-responsive nanogels of poly[2-(dimethylamino) ethyl methacrylate] by heterophase and microemulsion polymerization using gamma radiation. Polym Eng Sci 54:1625–1631
9. Oh JK, Siegwart DJ, Lee HI, Sherwood G, Peteanu L, Hollinger JO, Kataoka K, Matyjaszewski K (2007) Biodegradable nanogels prepared by atom transfer radical polymerization as potential drug delivery carriers: synthesis, biodegradation, in vitro release, and bioconjugation. J Am Chem Soc 129:5939–5945
10. Oh JK, Bencherif SA, Matyjaszewski K (2009a) Atom transfer radical polymerization in inverse miniemulsion: a versatile route toward preparation and functionalization of microgels/nanogels for targeted drug delivery applications. Polymer 50:4407–4423
11. Bhuchar N, Sunasee R, Ishihara K, Thundat T, Narain R (2012) Degradable thermoresponsive nanogels for protein encapsulation and controlled release. Bioconjug Chem 23:75–83
12. Averick SE, Magenau AJD, Simakova A, Woodman BF, Seong A, Mehl RA, Matyjaszewski K (2011) Covalently incorporated protein-nanogels using AGET ATRP in an inverse miniemulsion. Polym Chem 2:1476–1478
13. Oh JK, Lee DI, Park JM (2009b) Biopolymer-based microgels/nanogels for drug delivery applications. Prog Polym Sci 34:1261–1282
14. Klinger D, Landfester K (2011) Dual stimuli-responsive poly(2-hydroxyethyl methacrylate-*co*-methacrylic acid) microgels based on photo-cleavable cross-linkers: pH-dependent swelling and light-induced degradation. Macromolecules 44:9758–9772
15. McAllister K, Sazani P, Adam M, Cho MJ, Rubinstein M, Samulski RJ, DeSimone JM (2002) Polymeric nanogels produced via inversion microemulsion polymerization as potential gene and antisense delivery agents. J Am Chem Soc 124:15198–15207
16. Sanson N, Rieger J (2010) Synthesis of nanogels/microgels by conventional and controlled radical crosslinking copolymerization. Polym Chem 1:965–977
17. Yildrim T, Rinkenauer AC, Weber C, Traeger A, Schubert S, Schubert US (2015) RAFT made methacrylate copolymers for reversible pH-responsive nanoparticles. J Polym Sci Pol Chem 53:2711–2721
18. Gao H, Matyjaszewski K (2008) Synthesis of star polymers by a new "core-first" method: sequential polymerization of cross-linker and monomer. Macromolecules 41:1118–1125
19. Bencherif SA, Washburn NR, Matyjaszewski K (2009) Synthesis by AGET ATRP of degradable nanogel precursors for in situ formation of nanostructured hyaluronic acid hydrogel. Biomacromolecules 10:2499–2507
20. Graff RW, Shi Y, Wang X, Gao H (2009) Comparison of loading efficiency between hyperbranched polymers and cross-linked nanogels at various branching densities. Macromol Rapid Commun 36:2076–2082
21. Landfester K, Willert M, Antonietti M (2000) Preparation of polymer particles in nonaqueous direct and inverse miniemulsions. Macromolecules 33:2370–2376
22. Capek I (2010) On inverse miniemulsion polymerization of conventional water-soluble monomers. Adv Colloid Interf Sci 156:35–61
23. Dou XQ, Feng CL (2017) Amino acids and peptide-based supramolecular hydrogels for three-dimensional cell culture. Adv Mater 29:1604062
24. Svobodová J, Proks V, Karabiyik Ö, Koyuncu ACÇ, Köse GT, Rypáček F, Studenovská H (2017) Poly(amino acid)-based fibrous scaffolds modified with surface-pendant peptides for cartilage tissue engineering. J Tissue Eng Regen Med 11:831–842
25. Park CW, Yang HM, Woo MA, Lee KS, Kim JD (2017) Completely disintegrable redox-responsive poly(amino acid) nanogels for intracellular drug delivery. J Ind Eng Chem 45:182–188
26. Wu DQ, Cui HC, Zhu J, Qin XH, Tie T (2016) Novel amino acid based nanogel conjugated suture for antibacterial application. J Mater Chem B 4:2606–2613

27. Pitarresi G, Tomarchio V, Cavallaro G, Giammona G (1996) α,β-poly(*N*-hydroxy)-DL-aspartamide hydrogels as drug delivery devices. J Bioact Compat Polym 11:328–340
28. Giammona G, Pitarresi G, Tomarchio V, Cacciaguerra S, Govoni P (1997) A hydrogel based on a polyaspartamide: characterization and evaluation of in-vivo biocompatibility and drug release in the rat. J Pharm Pharmacol 49:1051–1056
29. Mandracchia D, Pitarresi G, Palumbo FS, Carlisi B, Giammona G (2004) pH-sensitive hydrogel based on a novel photocross-linkable copolymer. Biomacromolecules 5:1973–1982
30. Rypáček F, Drobnik J, Chmelař V, Kálal J (1982) The renal excretion and retention of macromolecules. The chemical structure effect. Pflügers Arch 392:211–217
31. Bae JW, Choi JH, Lee Y, Park D (2015) Horseradish peroxidase-catalysed in situ-forming hydrogels for tissue-engineering applications. J Tissue Eng Regen Med 9:1225–1232
32. Neri P, Antoni G, Benvenuti F, Cocola F, Gazzei G (1973) Synthesis of α,β-poly [(2-hydroxyethyl)-DL-aspartamide], a new plasma expander. J Med Chem 16:893–897
33. Jakeš J (1995) Regularized positive exponential sum (REPES) program—a way of inverting Laplace transform data obtained by dynamic light scattering. Collect Czechoslov Chem Commun 60: 1781–1797
34. Cavallaro G, Pitarresi G, Giammona G (2004) Advanced biomaterials for medical applications. Kluwer Academic Publishers, Dordrecht
35. Coviello T, Yuguchi Y, Kajiwara K, Giammona G, Cavallaro G, Alhaique F, Palleschi A (1998) Conformational analysis of α,β-poly(*N*-hydroxyethyl)-DL-aspartamide (PHEA) and α,β-polyasparthydrazide (PAHy) polymers in aqueous solution. Polymer 39:4159–4164
36. Jansen TGT, Meuldijk J, Lovell PA, van Herk AM (2016) On the miniemulsion polymerization of very hydrophobic monomers initiated by a completely water-insoluble initiators: thermodynamics, kinetics, and mechanism. J Polym Sci Polym Chem 54:2731–2745
37. Filipe V, Hawe A, Jiskoot W (2010) Critical evaluation of nanoparticle tracking analysis (NTA) by NanoSight for the measurement of nanoparticles and protein aggregates. Pharm Res 27:796–810
38. Gonzáles de Torre I, Quintanilla L, Pinedo-Martín G, Alonso M, Rodríguez-Cabello JC (2014) Nanogel formation from dilute solutions of clickable elastine-like recombinamers and its dependence on temperature: two fractal gelation modes. ACS Appl Mater Interfaces 6:14509–14515
39. Wang R, Xu DI, Liang L, Xu TT, Liu W, Ouyang PK, Chi B, Xu H (2016) Enzymatically crosslinked epsilon-poly-L-lysine hydrogels with inherent antibacterial properties for wound infection prevention. RSC Adv 6:8620–8627
40. Koul V, Mohamed R, Kuckling D, Adler HJP, Choudhary V (2011) Interpenetrating polymer network (IPN) nanogels based on gelatin and poly(acrylic acid) by inverse miniemulsion technique: synthesis and characterization. Colloid Surf B 83:204–213
41. Wu C, Böttcher C, Haag R (2015) Enzymatically crosslinked dendritic polyglycerol nanogels for encapsulation of catalytically active proteins. Soft Matter 11:972–980